The role played by the molecular weight and acetylation degree in modulating the stiffness and elasticity of chitosan gels

Pasquale Sacco[a,*], Michela Cok[a], Fioretta Asaro[b], Sergio Paoletti[a], Ivan Donati[a]

[a] *Department of Life Sciences, University of Trieste, Via Licio Giorgieri 5, I-34127 Trieste, Italy*
[b] *Department of Chemical and Pharmaceutical Sciences, University of Trieste, Via Licio Giorgieri 1, I-34127 Trieste, Italy*

ARTICLE INFO

ABSTRACT

A broad library of chitosans was produced varying the molecular weight and the fraction of acetylated units, F_A. The produced chitosans were used for the formation of wall-to-wall cylindrical gels through a controlled external gelation using tripolyphosphate (TPP) as cross-linker. The resulting gels were analyzed by rheometry. Viscosity average degree of polymerization ($\overline{DP_v}$) > 152 was shown to be required for the formation of stable gels. Both gel stiffness and gel rupture strength were proportional to the molecular weight regardless of the applied deformation. Increasing acetylation produced a marked reduction of the shear modulus, but, in parallel, switched the networks from rigid and brittle to weak and elastic. Intriguingly, gels made of chitosan with $F_A = 0.37$ displayed notable elasticity, *i.e.* up to 90% of applied strain falls into linear regime. These findings suggest that the frequency of glucosamine (D unit) and *N*-acetyl-glucosamine (A unit) contribute to a subtle structure-property relationship in chitosan-TPP gels.

1. Introduction

In tissue engineering, biomaterials can be conceived as scaffolds to mimic the extracellular matrix (ECM), and their interplay with cells is one of the key aspects to consider when designing such networks. In fact, cells require a suitable niche enabling survival and self-renewal. In this scenario, cells colonize biomaterials, interact with them and respond to the network physical composition to different extent. In general, internal contractile forces (generated by cytoskeleton remodeling when cells anchoring to substrates) depend on the external mechanical response given by the stiffness and elasticity of the surrounding microenvironment (Chaudhuri et al., 2015; Discher, Mooney, & Zandstra, 2009; Discher, Janmey, & Wang, 2005; Dupont et al., 2011; Engler, Sen, Sweeney, & Discher, 2006; Sen, Engler, & Discher, 2009).

Chitosans, as several other polymers of natural origin, have been used in the latest years as biomaterials in the field of tissue engineering. Chitosan is a collective name of a family of binary hetero-polysaccharides composed of β–1 → 4 linked 2-acetamido-2-deoxy-β-D-glucopyranose (GlcNAc, A unit) and 2-amino-2-deoxy-β-D-glucopyranose (GlcNH$_2$, D unit) residues, present in different relative proportion and sequence in the chain. Chitin, the structural component of the exoskeleton of arthropods and crustaceans and the second most abundant polysaccharide on earth, can be conveniently deacetylated under homogeneous and heterogeneous conditions to produce chitosans with

a random distribution of the two monomeric building sugars (Vårum, Anthonsen, Grasdalen, and Smidsrød, 1991b). Conversely, a random arrangement of units can be also achieved *via N*-acetylation of highly deacetylated chitosans using homogeneous conditions. (Sorlier, Denuzière, Viton, & Domard, 2001) Overall, partially *N*-acetylated chitosans are water-soluble polysaccharides with a range of the fraction of acetylated units, F_A, ranging from approximately 0.7 to almost 0. Chitosans are considered as low-toxic, non-immunogenic, biodegradable polysaccharides endowed with antibacterial and wound-healing activity (Nilsen-Nygaard, Strand, Vårum, Draget, & Nordgård, 2015).

Recently, the gelling properties of chitosan have been matter of discussion. (Nilsen-Nygaard et al., 2015; Racine, Texier, & Auzély-Velty, 2017) Ionic gelation and covalent cross-linking are the two most common methods for developing chitosan gels, albeit other examples are extensively reviewed in Reference (Racine et al., 2017). Among them, ionic gelation is perhaps the most appealing approach owing to lower toxicity of the resulting systems, tunable gel swelling extent and rate, mechanical behavior and degradation. Multivalent phosphate anions as tripolyphosphate (TPP) or pyrophosphate (PPi), polyol-phosphates and negatively charged sugar oligomers have been used as gelling agents to obtain physical chitosan gels with tunable mechanical properties (Khong, Aarstad, Skjåk-Bræk, Draget, & Vårum, 2013; Sacco et al., 2014, 2016; Supper et al., 2013).

Remarkable efforts have been made to achieve adequate

---

comprehension of the mechanism leading to ionic gelation or of the role played by parameters as polymer and cross-linker concentration. Still, a full understanding of the correlation between the physical/chemical features of chitosan and the mechanical properties of resulting gels is still lacking. Hence, it is of paramount importance to shed light onto this aspect, recalling the demonstrated importance of both molecular weight, (Draget, Simensen, Onsøyen, & Smidsrød, 1993; Kong, Lee, & Mooney, 2002; Smidsrød & Haug, 1972) and polymer chemical composition (Donati et al., 2005; Mørch, Holtan, Donati, Strand, & Skjåk-Bræk, 2008; Mørch, Donati, Strand, & Skjåk-Bræk, 2007; Kong, Emma Wong, & Mooney, 2003) in affecting the gel mechanical behavior of another heteropolysaccharide, *i.e.* alginate.

To contribute addressing these questions, we undertook a study to evaluate the influence of molecular weight and acetylation degree on the synthesis and mechanical properties of chitosan gels. A partially acetylated chitosan with medium molecular weight was selected and systematically modified *via* nitrous acid depolymerization (to vary the molecular weight, MW) and re-*N*-acetylation processes (to vary the acetylation degree) in order to create a library of polymers with different physical-chemical features. A chitosan with different molecular weight and similar F_A was chosen for comparison purposes. In this work, we report that different polymer characteristics led to a different behavior when cylindrical gels, synthetized through external gelation using TPP as cross-linker, underwent small/large deformations. Notably, we herein contribute to elucidating how molecular parameters can modulate chitosan gel stiffness, elasticity and rupture strength, with positive consequences for the development of chitosan-based biomaterials for potential application in tissue engineering and mechanotransduction.

2. Materials and methods

2.1. Materials

Novamatrix/FMC Biopolymer (Sandvika, Norway) kindly provided the chitosans used in this study. For convenience, they are indicated in the manuscript as chitosan A and chitosan B. Chitosan A was in base-form ($GlcNH_2$) whereas chitosan B was in its chloride salt ($GlcNH_2 \cdot HCl$). The physical-chemical features of all chitosans used in this work were determined by viscosity, ^{1}H NMR (Table 1) and ^{13}C NMR measurements. Sodium tripolyphosphate pentabasic – $Na_5P_3O_{10}$ – ($TPP \geq 98.0\%$), sodium chloride, acetic anhydride, sodium nitrite ($NaNO_2$), deuterium oxide (D_2O) and deuterium chloride (DCl) were all purchased from Sigma-Aldrich Chemical Co. Sodium borohydride ($NaBH_4$) was from Acros Organics. Sodium acetate (AcNa), acetic acid (AcOH), hydrochloric acid and ethanol were from Carlo Erba. Deionized water was used in all preparations.

2.2. Physical-chemical characterization of chitosans

The intrinsic viscosity [η] of chitosans was measured at 25 °C by means of a CT 1150 Schott Geräte automatic measuring apparatus and a Schott capillary viscometer. A buffer solution composed by 20 mM AcOH/AcNa, pH 4.5, and 100 mM NaCl was used as solvent. (Berth & Dautzenberg, 2002) Polymers were filtered through 0.45 μm Millipore (Germany) nitrocellulose filters prior to the measurements. Intrinsic viscosity was calculated by analyzing the polymer concentration dependence of the reduced specific viscosity, η_{sp}/c, and of the reduced logarithm of the relative viscosity, $\ln(\eta_{rel})/c$, by using the Huggins (1) and Kraemer (2) equations, respectively:

$$\frac{\eta_{sp}}{c} = [\eta] + k[\eta]^2 c \tag{1}$$

$$\frac{\ln \eta_{rel}}{c} = [\eta] - k'[\eta]^2 c \tag{2}$$

where k and k' are the Huggins and Kraemer constants, respectively. The intrinsic viscosity values were averaged. The corresponding viscosity average molecular weight ($\overline{M}_v$) of both chitosans was calculated in agreement to the Mark-Houwink-Sakurada equation (Eq. (3)).

$$[\eta] = K \cdot \overline{M}_v^a \tag{3}$$

where K and a parameters are 8.43×10^{-3} and 0.92, respectively. (Berth & Dautzenberg, 2002)

The fraction of acetylated units (F_A) was determined by ^{1}H NMR. Chitosan samples were prepared as follows: 20 mg of polymer were solubilized in 2 mL of D_2O + 150 μL of DCl under vigorous stirring and mild heating. Then, 30 μL of $NaNO_2$ 10 mg/mL were added and the solutions stirred for 2 h. Finally, 700 μL of chitosan samples were transferred into NMR tubes and analyzed by means of a JEOL EX-270 NMR spectrometer (6.3 T). The physical-chemical characteristics of chitosan A and B are summarized in Table 1.

The fraction of dyads was determined by ^{13}C NMR. Chitosan samples in a range of concentration 16–20 mg/mL were solubilized in HCl 70 mM and 20% v/v D_2O. Then, $NaNO_2$ was added (40 mg $NaNO_2$/g chitosan), and solutions stirred for 4 h. Finally, the pH was raised up to 5 with NaOH 5 M and solutions transferred into NMR tubes. The ^{13}C NMR measurements were carried out on a 500 VNMRS Varian NMR spectrometer operating at 125.63 MHz. The spectra were recorded at 80 °C. 34 000, 57 500 and 54 500 scans were accumulated for samples with $F_A = 0.14$, 0.37 and 0.49, respectively, using a spectral width of 25.510 kHz over 32 K complex point, with a recycle time of 1.5 s and a pulse width of 52° (Vårum, Anthonsen, Grasdalen, and Smidsrød, 1991a). The data were multiplied by a decaying exponential, with broadening factor of 3 Hz, and zero filled prior to FT. The dyad distributions were obtained from the integral ratios of Lorentzian lineshapes fitted to the experimental signals of C-6 by means of the Solver routine of Microsoft Excel.

2.3. Modification of chitosans

2.3.1. Converting chitosans into chloride salts

Chitosan A in its base-form was solubilized under mild stirring using AcOH 0.5% v/v as solvent at a final concentration of 0.4% w/v. The resulting chitosan solution was dialyzed as follows: NaCl 0.2 M in HCl 32 μM, pH 4.5 (1 shift); HCl 32 μM, pH 4.5 (1 shift); deionized water: *n* shifts until the conductivity at 4 °C was below 3 μS/cm. The pH was adjusted to 4.5 using HCl 1 M and finally the solution was freeze-dried. All chitosans derived from nitrous acid degradation and re-acetylation processes (*see below*) were converted into their chloride salts as described above prior being used.

2.3.2. Varying F_A

Chitosan A was re-acetylated to a different extent following the protocol reported in (Freier, Koh, Kazazian, & Shoichet, 2005). Briefly, 360 mg of chitosan A were solubilized at a final concentration of 3% w/v under mild stirring using AcOH 2% v/v as solvent. Subsequently, chitosan solution was diluted with an equal volume of ethanol and

Table 1
Physical-chemical parameters of chitosans used in this study. The fraction of acetylated units, (F_A), was determined by means of ^{1}H NMR, whereas intrinsic viscosity, [η], was determined by viscometry. The viscosity average molecular weight, $\overline{M}_v$, was calculated in agreement to Mark-Houwink-Sakurada equation (see Eq. (3)), and $\overline{DP}_v$, *i.e.* the viscosity average degree of polymerization, stands for the ratio between $\overline{M}_v$ and the MW of the chitosan repeating unit, MW_{ru} (Note: $GlcNH_2 \cdot HCl$ was used for the calculation of MW_{ru}).

Sample	F_A	[η] (mL/g)	$\overline{M}_v$	MW_{ru}	$\overline{DP}_v$
chitosan A	0.14	988	320 000	197.8	1618
chitosan B	0.16	681	220 000	198.0	1111

Table 2

Molar ratio of acetic anhydride to glucosamine unit of chitosan A, R, in order to vary the fraction of acetylated units (F_A). F_A of resulting chitosans was determined by ^1H NMR.

R	F_A
0.063	0.24
0.120	0.28
0.177	0.33
0.234	0.37
0.354	0.49

vigorously stirred. Finally, required amounts of acetic anhydride were added, and solutions were stirred overnight. The molar ratio, R, between acetic anhydride and glucosamine unit, *i.e.* $R = [\text{anhydride}]/[\text{GlcNH}_2]$, was used as parameter to vary F_A (Table 2). At the end of reaction, chitosans were converted into their chloride form as described above and freeze-dried. F_A of resulting chitosans was determined by means of ^1H NMR.

2.3.3. Varying molecular weight

Chitosan A was depolymerized by means of nitrous acid degradation. Briefly, 200 mg of chitosan A were solubilized at a concentration of 0.93% w/v under mild stirring using HCl 70 mM as solvent and at a final volume of 21.5 mL. Then, 300 μL of $NaNO_2$ at different concentration (based on the desired depolymerization degree) were added and solutions stirred for 30 min pH was adjusted in the range 4–5 and 2 mL of 6% w/v $NaBH_4$ were added. Resulting chitosan solutions were stirred overnight. Finally, chitosans were converted into their chloride salts as described above and freeze-dried. The extent of depolymerization was calculated by means of viscosity measurements as above described.

2.4. Chitosan gel preparation

Wall-to-wall cylindrical gels were obtained by the slow ion diffusion technique reported in (Sacco et al., 2014) with some modifications. 66 mg of hydrochloride chitosans, together with 2.2 g of deionized water (3% w/v final concentration), were weighed into 5 mL beaker and stirred until complete polymer solubilization. Chitosan solutions were stored at 4 °C overnight and casted into a mold (diameter = 22 mm, thickness = 2.5 mm) closed by two dialysis membranes (average flat width 33 mm with a cut-off of 14 000 or average flat width 32 mm, benzoylated, with a cut-off of 2 000, Sigma Aldrich, Chemical Co., U.S.A.) and fixed by double circular stainless iron rings. The system was hermetically sealed and immersed into a gelling solution of TPP. The concentration of TPP in the gelling solution was varied based on chemical composition (F_A) of each chitosan, thus the molar ratio (r) between the cross-linker and repeating unit of chitosan ($r = [\text{TPP}]/[\text{chitosan}]_{\text{r.u.}}$) was set to 5.2 at the beginning of the dialysis (Sacco et al., 2016). The pH of the TPP-containing gelling solution was adjusted to 4.50 ± 0.02 using HCl 5 M, and buffer AcOH/AcNa was added (1 mM final concentration). The corresponding value of the (positive) charge fraction per chitosan repeating unit (β) was calculated to be approximately 0.97 (α = 0.03) in the case of chitosan with $F_A = 0.14$ and 0.16, whereas β = 1 for chitosan samples with $F_A > 0.16$ (Sorlier et al., 2001). Ion diffusion proceeded for 24 h under moderate stirring at room temperature allowing for gel formation.

2.5. Rheological measurements

Rheological characterization of chitosan gels was performed by means of a controlled stress rheometer HAAKE MARS III operating at 25 °C using a shagreened plate-plate apparatus ("HPP20 *profiliert*":

diameter = 20 mm) as the measuring device. To avoid water evaporation from the gel, measurements were performed in a water-saturated environment formed by using a glass bell (solvent trap) containing a wet cloth. In addition, to prevent both wall-slippage and excessive gel squeezing, the gap between plates was adjusted by executing a series of short stress sweep tests ($\nu = 1$ Hz; stress range 1–5 Pa) until a constant G' was reached. Based on these preliminary results, the selected gap was set to 2.4 mm for all gels investigated. For each gel, the linear viscoelastic range was determined by means of stress sweep tests consisting in measuring elastic (G') and viscous (G″) moduli variation with increasing shear stress (1 Pa $< \tau <$ 1 000 Pa) at a frequency $\nu = 1$ Hz (hence with $\omega = 2\pi\nu = 6.28$ rad/s). The mechanical spectra (frequency sweep tests) of gels were recorded by measuring the dependence of the elastic (G') and viscous (G″) moduli on pulsation ω at constant shear stress $\tau = 5$ Pa (well within the linear viscoelastic range).

2.6. Evaluation of syneresis

Syneresis (as water loss) was determined as the weight reduction of chitosan gels with respect to the initial weight, the latter given by the sum of polymer and water masses and assuming a density value of 1. After external gelation, gels were taken out from the mold and weighed. The % syneresis was calculated as $(1 - W/W_0) \times 100$, where W and W_0 are the final and initial weight of the gel cylinders, respectively.

2.7. Evaluation of homogeneity

The distribution of chitosan within the gels was analyzed by confocal microscopy (Nikon Eclipse C1si confocal laser scanning microscope using a 4x as objective). Gels were synthetized using 10% w/w of FITC-labelled polymer, prepared as previously described (Sacco et al., 2018). The gels were sectioned and the fluorescent signal was acquired on the cross section (gelling axis) from edge to edge of the samples (excitation wavelength: 488 nm; emission wavelength: 515 nm). Image analysis was carried out by the software ImageJ in order to measure the fluorescence intensity profiles along the gelling axis. Five replicates were averaged for the analysis.

3. Results and discussion

3.1. Effect of molecular weight

To evaluate the role played by molecular weight in the formation of macroscopic chitosan gels and on their mechanical properties, chitosan A was systematically degraded whereas chitosan B was used as such. In order to obtain chitosan samples of different molecular weights with approximately the same type of molecular weight distribution, nitrous acid depolymerization was used as the degradation method. Nitrous acid randomly cleaves chitosan's backbone in correspondence of D units, thus generating reactive 2,5-anhydro-D-mannose residues (also termed M units) as new reducing ends. (Allan & Peyron, 1989; Tømmeraas, Vårum, Christensen, & Smidsrød, 2001) Unstable M sugars were reduced conventionally by sodium borohydride treatment.

Viscosity measurements were performed to measure the depolymerization of chitosan. Since this reaction is stoichiometric with respect to the amount of nitrous acid used, the number of cleaved glycosidic bonds was expected to increase upon increasing sodium nitrite amount, yielding lower molecular weight chitosans. As a matter of these considerations, two weight-ratios between sodium nitrite and chitosan were selected, namely 3 or 15 mg $NaNO_2$/g chitosan, and resulting degraded polysaccharides were analyzed by viscometry. The calculated intrinsic viscosities, $[\eta]$, were 405 and 105 mL/g, respectively, with estimated viscosity average molecular weights, $\overline{M_v}$, of 120 000 and 30 000, respectively. Furthermore, by assuming the same chemical composition of chitosan A, the calculated viscosity average degree of polymerization, $\overline{DP_v}$, was 607 and 152, respectively.

Original and degraded chitosans were dialyzed against TPP to obtain wall-to-wall gels following a procedure previously reported (Sacco et al., 2014). It was found that chitosan with intrinsic viscosity of 105 mL/g did not allow the formation of continuous cylindrical networks, but, rather, rigid surface layers and a liquid-like core were observed. These findings are in line with other gelling systems (Skjåk-Bræk, Grasdalen, & Smidsrød, 1989). In the used procedure, two concentration gradients are formed: the first one is the gradient of the gelling agent (presently, TPP) toward the polymer solution compartment. In the opposite direction, a polymer gradient is built up. They are mutually correlated, but the polymer gradient is clearly much more dependent on the diffusion coefficient of the large macromolecule and on the possibility that a rapid formation of a dense 3D network over the whole volume hinders the further diffusion of chitosan chains towards the gel boundary. Both events strongly depend on the chain dimension, *i.e.* on MW. High MW polyelectrolytes create a gel network with high connectivity preventing the easy migration of long chains, which, over and above, would diffuse slowly because of their high viscosity. This combined effect hinders the formation of a marked gelling gradient and, in turn, allows for a more homogeneous distribution of TPP throughout the polymer. Low MW polymers would move much faster (due to lower viscosity) and would display a much lower capability-per-chain of making gel junctions. Hence, it seems that at least $\overline{DP_v} > 152$ was mandatory for the formation of wall-to-wall chitosan networks. Our results slightly differ from the alginate-Ca^{+2} system, where a minimum value of $\overline{DP_v}$ (*i.e.* 70) was calculated in similar experimental conditions for gel formation, *i.e.* in terms of polymer concentration, C_p ($C_p = 3\%$) and method (external gelation) (Smidsrød & Haug, 1972). It seems reasonable to propose that the comparatively lower overall propensity of chitosan-TPP toward ionic gelation with respect to that of the alginate-Ca^{+2} system can be traced back to the lower effective charge density of the former polysaccharide.

Chitosans with higher degree of polymerization allowed the formation of wall-to-wall cylindrical gels, albeit a slight inhomogeneity was detected in the case of gels made of $\overline{DP_v} = 607$ chitosan (Fig. S1), in line with what discussed above. Conversely, higher molecular weight chitosans are well known to promote the formation of much more homogeneous systems (Sacco et al., 2018, 2016). Rheological measurements were carried out to evaluate the mechanical properties of this set of materials. Mechanical spectra in a range of pulsation, ω, from 0.01 to 100 rad/s showed that G' exceeded of approximately one order of magnitude G″ in the whole range of investigated frequencies (given $\omega = 2\pi\nu$), thereby classifying such networks as "strong gels" (Fig. 1A). Secondly, for all gels analyzed both G' and G″ experimental points were efficiently fitted by a combination of Maxwell elements, composed by a sequence of springs and dashpots in parallel *plus* a pure elastic spring, G_e, according to (4) and (5), (Sacco et al., 2014)

$$G' = G_e + \sum_{i=1}^{n} G_i \frac{(\lambda_i\omega)^2}{1 + (\lambda_i\omega)^2}; \; G_i = \frac{\eta_i}{\lambda_i} \tag{4}$$

$$G'' = \sum_{i=1}^{n} G_i \frac{\lambda_i\omega}{1 + (\lambda_i\omega)^2}; \; G_i = \frac{\eta_i}{\lambda_i} \tag{5}$$

where n is the number of Maxwell elements considered, G_i, η_i and λ_i represent the spring constant, the dashpot viscosity and the relaxation time of ith Maxwell element, respectively. The number of the Maxwell elements was selected based on a statistical procedure to minimize the product $\chi^2 \times N_p$, where χ^2 is the sum of the squared errors, while N_p ($= 2 + n$) indicates the number of fitting parameters. The fitting of the experimental data was performed assuming that relaxation times are not independent of each other but they are scaled by a factor 10.

The use of Maxwell model enabled to calculate the shear modulus, G, (6) which reflects the stiffness of gels under a constant stress at small deformations.

$$G = G_e + \sum_{i=1}^{n} G_i \tag{6}$$

As expected, it was found that the shear modulus increased with increasing $\overline{DP_v}$ of chitosan, *i.e.* molecular weight (Fig. 1B). These results are in line with those of Smidsrød et al. on Ca^{2+}-alginate system (Smidsrød & Haug, 1972; Draget et al., 1993), albeit some considerations are worthy to be drawn. Specifically, in the quoted cases a different dependence of the mechanical behavior on molecular weight was noticed depending upon the method used for the synthesis of gels. In particular, the dependence on molecular weight was higher for calcium-limited gels (*i.e.* obtained by internal gelation) than for saturated gels (*i.e.* obtained by dialysis). In our case, we found that the trend for chitosan-TPP gels closely resembles that of alginate-Ca^{+2} gels fabricated *via* internal gelation, even though they were produced by dialysis. Such a behavior could reasonably stem from the different modality of binding of TPP to chitosan at variance with that of calcium to alginate, where the known egg-box model takes place.

Stress sweep tests were carried out at constant frequency of 1 Hz while progressively increasing the strain. Experimental data in Fig. 2A show that the elastic modulus for all chitosan gels with different $\overline{DP_v}$ values is independent of deformation up to approximately $\gamma = 0.01$. Beyond $\gamma = 0.01$, a marked deviation from linearity was observed ("type-I" gel behavior). Specifically, both a decrease of G' and an increase of phase angle (δ) were found, thereby indicating the onset of strain softening, potentially resulting in gel fracture for larger strain values. Experimental points were efficiently fitted by the Soskey-Winter equation (Soskey & Winter, 1984) (7)

$$G' = G'_0 \frac{1}{1 + (b\gamma)^n} \tag{7}$$

where G'_0 is the limiting value of the storage modulus for $\gamma \to 0$, while b and n are adjustable parameters. The critical strain, γ_c, which herein
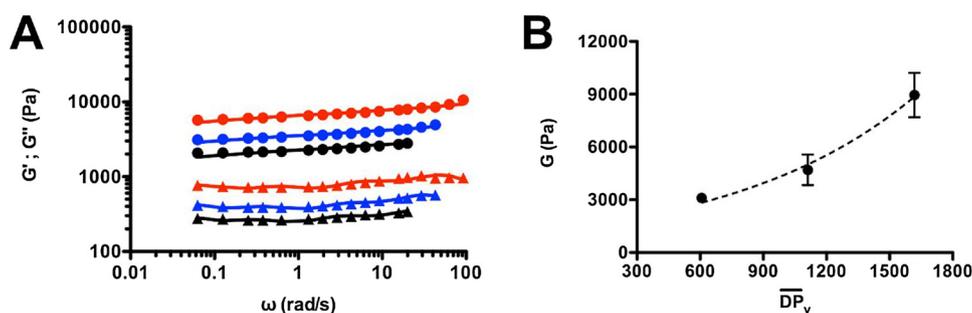
Fig. 1. (A) G' (circles) and G″ (triangles) for chitosan-TPP gels synthetized with different viscosity average degree of polymerization chitosans: $\overline{DP_v} = 1618$ (red), 1111 (blue) and 607 (black); solid lines represent the best fitting of G' and G″ experimental points using the Maxwell model. (B) Dependence of the shear modulus, G, ($\pm$ SD, $n = 3$) on $\overline{DP_v}$; dashed line is drawn to guide the eye. (For interpretation of the references to colour in this figure legend, the reader is referred to the web version of this article.)

found that the critical strain slightly decreased (anyhow within experimental error) with increasing the molecular weight, ranging from 0.017 ± 0.003 to 0.012 ± 0.002 for chitosans with $\overline{DP_v}$ equal to 607 and 1618, respectively. Conversely, the corresponding critical stress, τ_c, at γ_c increased with increasing polymer molecular weight (anyhow within experimental error), being 51 ± 13, 64 ± 12 and 96 ± 35 Pa for chitosans with $\overline{DP_v}$ equal to 607, 1111 and 1618, respectively.

To further evaluate the strength of gels made of chitosans with different molecular weight, the work at γ_c, W_{G,γ_c}, was calculated as (8):

$$W_{G,\gamma_c} = \int_0^{\gamma_c} \tau d\gamma$$

(8)

The energy required to elicit the onset of strain softening was found to increase with increasing $\overline{DP_v}$ (Fig. 2C), albeit in a fashion less dependent on $\overline{DP_v}$ than the shear modulus (Fig. 1B). These findings can be justified considering the different contribution of elastic (entrapped chains) and non-elastic chains (loose ends) within gels. When chitosan with $\overline{DP_v} = 607$ is considered, resulting networks display a reduced number of stable intermolecular junctions together with a higher amount of non-elastic chains giving weak gels (Figs. 1B and 2C). Conversely, a larger amount of stable inter-chain cross-links and a reduction of non-elastic stretches are expected to exist in higher molecular weight chitosans gels, thereby giving very stiff gels, which require higher amounts of energy to foster the onset of gel breaking. Our results are again in line with those of Draget et al. (1993) Overall, we can conclude that medium/high molecular weight chitosans ($\overline{M_v} \geq 120\,000$) guarantee the formation of gels endowed with tunable rigidity and gel rupture strength.

3.2. Effect of acetylation degree

To evaluate the role of chemical composition on the formation and mechanical properties of gels, chitosan A (with $\overline{DP_v} = 1618$) was systematically re-N-acetylated using acetic anhydride as the acetyl group donor. Although the addition of acetyl groups to chitosan backbone slightly alters the final molecular weight of the polymer (approximately 1%), the contribution of $-COCH_3$ grafting was considered negligible for the interpretation of results. ^1H NMR spectra of re-acetylated samples were recorded for the determination of relative F_A (Table 2).

Chitosan A and re-acetylated samples were dialyzed against TPP to obtain cylindrical gels. As a general consideration, all re-acetylated chitosans allowed for the formation of cylindrical networks, suggesting that a reduction of reactive $-NH_3^+$ groups from 86 to 51% did not hamper the complete wall-to-wall gelation.

Since the chitosan-TPP gelling system belongs to the category of ionic gels, one may expect that a reduction of positive charges on chitosan generated by acetyl group addition would cause a decrement of the stiffness for chitosan gels with lower F_D. To shed light onto this aspect, the dependence of the storage and loss moduli on pulsation was recorded. Mechanical spectra in Fig. 3A show that (i) G' exceeds G″ by approximately one order of magnitude for the whole range of frequencies investigated and that (ii) G' progressively increases upon increasing F_D. Maxwell model was used for the calculation of the shear

Fig. 2. (A) Dependence of the elastic modulus, G', (circles) and phase angle, δ, (triangles) on strain for chitosan-TPP gels synthetized with different viscosity average degree of polymerization chitosans: $\overline{DP_v}$ = 1618 (black), 1111 (red) and 607 (blue); solid lines represent the best fitting of the elastic modulus experimental points using Soskey-Winter model. (B) Dependence of the critical strain, γ_c, ($\pm$ SD, n = 3) on $\overline{DP_v}$; dashed line is drawn to guide the eye. (C) Dependence of the work at critical strain, W_{G,γ_c}, ($\pm$ SD, n = 3) on $\overline{DP_v}$; dashed line is drawn to guide the eye. (For interpretation of the references to colour in this figure legend, the reader is referred to the web version of this article.)

indicates the limit of the linear regime, was arbitrarily calculated as $\gamma_c = \frac{G'}{G'_0} = 0.95$. (Marsich et al., 2013) The trend of γ_c vs. $\overline{DP_v}$ for different molecular weight chitosan gels is reported in Fig. 2B. It was

Fig. 3. (A) G' (circles) and G″ (triangles) for chitosan-TPP gels synthetized with different fraction of deacetylated units chitosans: F_D = 0.86 (red), 0.72 (blue) and 0.51 (black); solid lines represent the best fitting of G' and G″ experimental points using Maxwell model. (B) Dependence of the shear modulus, G, ($\pm$ SD, n = 3) on F_D. Dashed line is drawn to guide the eye. (For interpretation of the references to colour in this figure legend, the reader is referred to the web version of this article.)

modulus, G, as described above. Fig. 3B shows that the modulus G of the considered samples increases with increasing F_D with the power law: $G \propto F_D^{5.3}$ ($R^2 = 0.95$).

Data have been obtained after 24 h of dialysis, necessary to allow for the gel formation. After that time, the weight of the gels at different F_D values was observed to depend on F_D. The different amount of water produces a difference in the effective polymer concentration in the gel, C_p. Gel strength strongly depends on C_p, even with a power dependence of 3 or more. (Sacco et al., 2014) Therefore, the data values in Fig. 3B may be systematically affected by an error due to different polymer concentration. A thorough study of water imbibition (or, conversely, water syneresis) was out of the scope of this investigation. Nevertheless, in an exploratory study (preliminary data not reported) it was observed that the water content of the chitosan-TPP gels was positively correlated with the degree of chitosan deacetylation, F_D. It means that the "effective" value of C_p is lower in the gels with higher F_D. Therefore, should any correction of the values of G be made to take into account the C_p effect, the results of Fig. 3B would even more strongly (and progressively) increase the value of G the larger the value of F_D. Overall, these results confirms that the shear modulus gradually increases upon increasing F_D, thus confirming our assumption, namely that a direct relationship between the availability of D units – representing the sites for TPP binding – and gel strength holds.

Long stress sweep experiments were carried out to study the dependence of G' at large deformations for different F_A chitosan gels. It was found that $F_A = 0.14$ and 0.37 chitosan gels behaved very differently (Fig. 4A–B). Specifically, deviation from linearity together with an increase of phase angle were noticed at approximately $\gamma = 0.02$ in the case of networks made of chitosan with $F_A = 0.14$ (Fig. 4A). Conversely, the elastic modulus was found to be almost constant in the range of the applied deformations for gels made of chitosan with $F_A = 0.37$. A markedly non-linear response − strain softening profile –

was identified for gels made of chitosan with $F_A = 0.14$. On the contrary, in the case of $F_A = 0.37$ the shear stress scaled almost linearly with the shear strain up to 87% of total deformation (so-called Gaussian behavior) (Zhang, Daubert, & Allen Foegeding, 2007), again pointing out the different behavior between the two systems, with a remarkable ability of $F_A = 0.37$ chitosan gels to withstand the deformation (Fig. 4C). The calculated values of γ_c confirmed that networks made of $F_A = 0.37$ chitosan displayed an evident increase of the elastic behavior with respect to other systems. Namely, γ_c was 0.012 ± 0.002 and 0.258 ± 0.008 for gels made of chitosan with $F_A = 0.14$ and $F_A = 0.37$, respectively. The dependence of γ_c on F_A is reported in Fig. 4D. γ_c slightly increased for chitosan networks up to $F_A = 0.28$, whereas it showed an abrupt increase when acetylation degree was raised further, up to $F_A = 0.37$. However, a drop of γ_c was found for chitosan gels with a further increase of F_A to 0.49, suggesting that the latter showed a lower elasticity with respect to gels made of chitosan with $F_A = 0.37$, albeit being greater than those of chitosan gels with $F_A < 0.33$.

Taken together, the results depicted in Figs. 3 and 4 allow drawing an intriguing scenario: the chemical composition of chitosans strongly affects the mechanical performance of gels synthetized *via* external gelation. More in detail, our findings reveal that the stiffness and the elasticity of networks are strictly depended on A and D content, respectively; very stiff and brittle systems were obtained when lower acetylated chitosans were used, while weak and more elastic gels were fabricated with higher acetylated chitosans. The dependence of critical strain up to $F_A = 0.37$ samples on the acetylation degree (Fig. 4D) closely resembles the case of alginate-Ca^{+2} system, where the elasticity was found to increase with increasing MG content (Mørch et al., 2007). Hence, it seems that the presence of A units which are not involved in the ionotropic gelation with TPP^{-3} ions, would be beneficial for the elasticity gain and, at the same time, detrimental for the rigidity
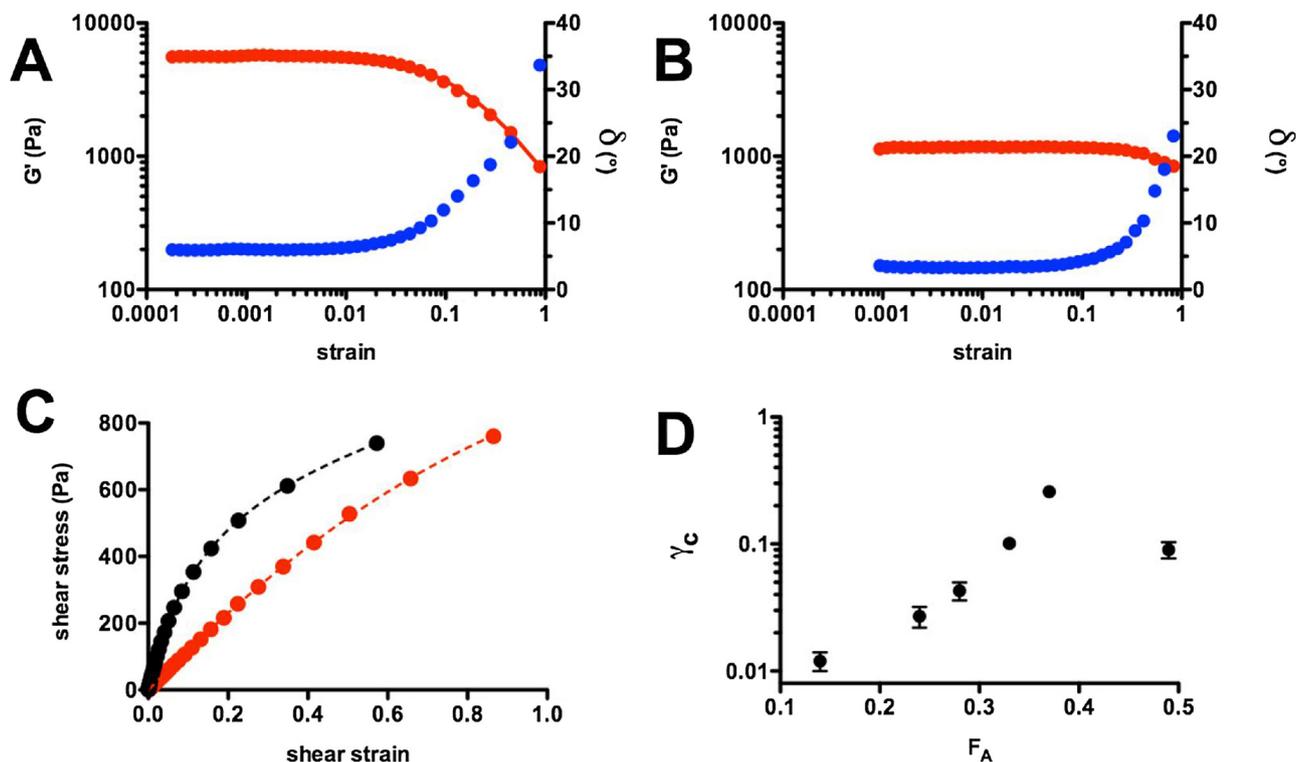
Fig. 4. (A–B) Dependence of the elastic modulus, G', (red circles) and phase angle, δ, (blue circles) on strain for chitosan-TPP gels synthetized with different fraction of acetylated units chitosans: (A) $F_A = 0.14$ and (B) 0.37; solid red lines represent the best fitting of the elastic modulus experimental points using Soskey-Winter model. (C) Dependence of the shear stress on the shear strain up to 100% of total deformation for chitosan-TPP gels synthetized with different fraction of acetylated units chitosans: $F_A = 0.14$ (black circles) and $F_A = 0.37$ (red circles); dashed lines are drawn to guide the eye. (D) Dependence of the critical strain, γ_c, ($\pm$ SD, $n = 3$) on F_A. (For interpretation of the references to colour in this figure legend, the reader is referred to the web version of this article.)

(stiffness) of gels.

The sequence of sugars along chitosan backbone, the cross-linking density and the length of cross-linking junctions have to be taken into account for the interpretation of the results as well (Zhang et al., 2007; Kong et al., 2003; Mørch et al., 2008; Donati et al., 2005). The number-average block length of D units, $\overline{N_D}$, was determined from ^{13}C NMR analysis (see Table S1 and Fig. S2), and resulted to be 7.8, 2.7 and 2.0 for chitosan samples with F_A = 0.14, 0.37 and 0.49, respectively. Hence, chitosan gels with F_A = 0.14 (meaning with a high D block content) would display higher cross-linking density per unit volume with respect to the more acetylated counterparts. As a result, very short and stiff elastic stretches between two cross-links are expected to exist.

Assuming that chitosan-TPP gels behave as ideal systems with regular mesh and punctual junctions (front factor φ = 1), Flory's and equivalent network theories allow computing the mole of cross-links per unit volume, ρ, (9):

$$\rho = \frac{G}{RT\varphi} \tag{9}$$

and the average network mesh size, $\bar{\xi}$, (Grassi, Farra, Fiorentino, Grassi, & Dapas, 2015) (10):

$$\bar{\xi} = \sqrt[3]{\frac{6}{\pi\rho N_A}} \tag{10}$$

where R is the universal gas constant, T the absolute temperature, G the shear modulus and N_A the Avogadro's number. The calculated values of cross-linking density and the distance between two consecutive junctions are reported in Fig. 5A for gels made of chitosans with different F_A values.

As expected, a progressive decrement of junction density per unit volume and a parallel increment of the distance between two consecutive cross-links were noticed upon increasing F_A (Fig. 5A). Bearing this in mind, it is likely that when small deformations are applied in the linear stress/strain region, the elevate number of elastically active chains in chitosan networks with F_A = 0.14, together with long and rigid D-D sequences within a singular junction, guarantee excellent strength to the gels (Fig. 3B). Conversely, junctions zones are expected to deform and progressively fracture at large deformations, thus causing energy transfer from one D unit to neighbor D sugars according to a cascade process, (Zhang et al., 2007) unzipping the junction in a co-operative manner. Clearly, the higher the length of $\overline{N_D}$, the higher the amplification of energy transfer.

Upon increasing the content of A blocks, a reduction of cross-linking density takes place and, in turn, a reduction of $\overline{N_D}$. Such a scenario may be correlated with the gain of rupture strength at large deformations ascribed to the dissipation of energy through A units (Scheme 1), or D units not involved in the formation of stable junctions, reasonably *via* sliding, (Mørch et al., 2008) or partial and stepwise de-cross-linking mechanisms. (Kong et al., 2003) Hence, larger amounts of energy are needed to evoke gel rupture.

Therefore, the very high value of γ_c observed in the case of chitosan gels with F_A = 0.37 and F_A = 0.49 (Fig. 4D) seems to indicate that in those cases (high F_A) a mechanism is active which is able to dissipate the energy applied by shear. This could be traced back to the presence of specific sequences containing some A residues, which are able not to hamper adaptive binding of TPP.

The work at γ_c was calculated according to (8) and subsequently normalized for the number of equivalent junctions, ρ, per unit volume (Fig. 5B) (Donati, Mørch, Strand, Skjåk-Bræk, & Paoletti, 2009). The energy required to allow a mole of equivalent junctions exiting from linear regime in different F_A chitosan gels showed a similar trend as γ_c (Fig. 4D), again pointing to the highest gel rupture strength of chitosan gels with F_A = 0.37 with respect to other systems made of lower F_A chitosans. The gels composed of chitosan with acetylation degree of 49% showed a drop of the $^{W_{G,\gamma_c}}/_\rho$ ratio from 89.2 ± 1.5 to 9.8 ± 4.0 J/mol. The work at critical strain resulted anyway considerably greater than that of chitosan gels with F_A = 0.14 (Fig. 5B). It is unlikely to believe that shorter junctions formed in chitosan networks with F_A = 0.49 endure better gel rupture than longer cross-links in chitosan gels with F_A = 0.14 if external gelation is considered (TPP-saturated conditions). This apparent inconsistency is overcome if, for the present case, the presence of energy dampers is postulated, similarly to other reported polysaccharide cases. In particular, these results are in line with those found for alginate with elongated MG sequences, which are known to bind Ca^{2+} in MG-MG junctions that act as weak reels embedded within the gel network (Donati et al., 2009).

The whole of the rheological results therefore unveil a subtle correlation between the number and type of sugars involved in the formation of energy dampers and the mechanical response of the resulting chitosan gels. It follows that such sequences would (*i*) unwind upon application of the stress – albeit still being able to provide some type of TPP interchain binding – and (*ii*) dissipate the energy, thus increasing the overall elasticity of gels before breaking.

4. Conclusions

Tuning mechanical properties of chitosan gels guarantees a powerful tool for customizing these biomaterials according to the desired purposes. In this work, a study to understand the role of chitosan molecular weight and polymer chemical composition on the formation and mechanical response of cylindrical gels synthetized *via* external gelation using TPP as the cross-linker has been undertaken. In the first section, we reported that:

(i) the complete wall-to-wall gelation of chitosans requires that the (average) molecular weight is larger than a threshold value;
(ii) the gel stiffness (calculated as the shear modulus at small deformations) as well as the gel rupture strength (calculated as the
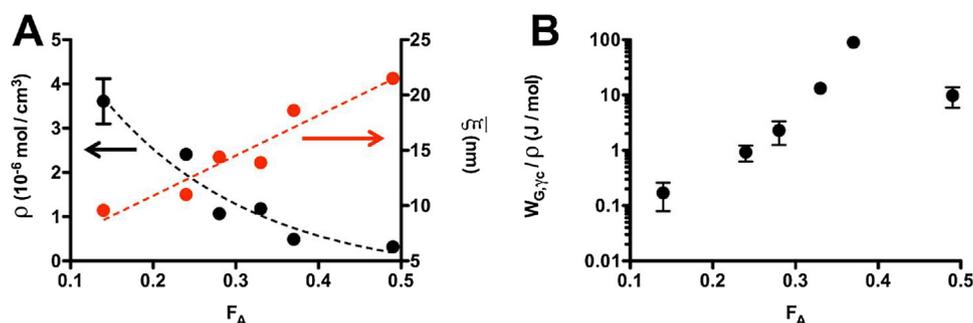
Fig. 5. (A) Dependence of the junction density per unit volume, ρ, (black circles) and the average network mesh size (*i.e.* the distance between two consecutive junctions), $\bar{\xi}$, (red circles) on the fraction of acetylated units (F_A); dashed lines are drawn to guide the eye; data are means (± SD, n = 3). (B) Dependence of the $^{W_{G,\gamma_c}}/_\rho$ ratio (work at critical strain on junction density per unit volume) on the fraction of acetylated units (F_A); data are means (± SD, n = 3). (For interpretation of the references to colour in this figure legend, the reader is referred to the web version of this article.)

energy required to elicit the onset of non-linear regime) increase with increasing molecular weight;

(iii) the elasticity (calculated as the limit of the linear viscoelastic regime) is almost independent of molecular weight.

In the second part of this contribution, we showed how varying the acetylation degree of chitosans it was possible to switch from very stiff and brittle to weaker but much more elastic gels. One of the striking findings of this work is the prominent gel rupture strength noticed for chitosan networks with $F_A = 0.37$, which were found to deform up to 90% of total strain without softening. These results indicate a precise balance of A and D unit content forming "energy dampers" and determining such a mechanical behavior. In this regard, the present contribution has laid the groundwork for necessary, forthcoming investigations.

Notes

The authors disclose any actual or potential conflict of interest.

Acknowledgments

Appendix A. Supplementary data

Supplementary data associated with this article can be found, in the online version, at https://doi.org/10.1016/j.carbpol.2018.05.060.

References

Allan, G. G., & Peyron, M. (1989). Chitin and chitosan: Sources, chemistry, biochemistry, physical properties, and applications. In G. SkjHk-Braek, T. Anthonsen, & P. Sandford (Eds.). *Chitin and chitosan: Sources, chemistry, biochemistry, physical properties, and applications* (pp. 443–466). London: Elsevier Science Publishers.

Berth, G., & Dautzenberg, H. (2002). The degree of acetylation of chitosans and its effect on the chain conformation in aqueous solution. *Carbohydrate Polymers, 47*(1), 39–51.

Chaudhuri, O., Gu, L., Klumpers, D., Darnell, M., Bencherif, S. A., Weaver, J. C., ... Mooney, D. J. (2015). Hydrogels with tunable stress relaxation regulate stem cell fate and activity. *Nature Materials, 15*(3), 326–334.

Discher, D. E., Janmey, P., & Wang, Y.-L. (2005). Tissue cells feel and respond to the stiffness of their substrate. *Science, 310*(5751), 1139–1143.

Discher, D. E., Mooney, D. J., & Zandstra, P. W. (2009). Growth factors, matrices, and forces combine and control stem cells. *Science (New York, N.Y.), 324*(5935), 1673–1677.

Donati, I., Holtan, S., Mørch, Y. A., Borgogna, M., Dentini, M., & Skjåk-Bræk, G. (2005). New hypothesis on the role of alternating sequences in calcium-alginate gels. *Biomacromolecules, 6*(2), 1031–1040.

Donati, I., Mørch, Y. A., Strand, B. L., Skjåk-Bræk, G., & Paoletti, S. (2009). Effect of elongation of alternating sequences on swelling behavior and large deformation properties of natural alginate gels. *The Journal of Physical Chemistry B, 113*(39), 12916–12922.

Draget, K. I., Simensen, M. K., Onsøyen, E., & Smidsrød, O. (1993). Gel strength of Ca-limited alginate gels made in situ. *Hydrobiologia, 260–261*(1), 563–565.

Dupont, S., Morsut, L., Aragona, M., Enzo, E., Giulitti, S., Cordenonsi, M., ... Piccolo, S. (2011). Role of YAP/TAZ in mechanotransduction. *Nature, 474*(7350), 179–183.

Engler, A. J., Sen, S., Sweeney, H. L., & Discher, D. E. (2006). Matrix elasticity directs stem cell lineage specification. *Cell, 126*(4), 677–689.

Freier, T., Koh, H. S., Kazazian, K., & Shoichet, M. S. (2005). Controlling cell adhesion and degradation of chitosan films by N-acetylation. *Biomaterials, 26*(29), 5872–5878.

Grassi, M., Farra, R., Fiorentino, S. M., Grassi, G., & Dapas, B. (2015). Hydrogel mesh size evaluation. In M. Pietro, A. Franco, & C. Tommasina (Eds.). *Polysaccharide hydrogels characterization and biomedical applications* (pp. 139–165). Pan Stanford.

Khong, T. T., Aarstad, O. A., Skjåk-Bræk, G., Draget, K. I., & Vårum, K. M. (2013). Gelling concept combining chitosan and alginate-proof of principle. *Biomacromolecules, 14*(8), 2765–2771.

Kong, H.-J., Lee, K. Y., & Mooney, D. J. (2002). Decoupling the dependence of rheological/mechanical properties of hydrogels from solids concentration. *Polymer, 43*(23), 6239–6246.

Kong, H. J., Emma Wong, A., & Mooney, D. J. (2003). Independent control of rigidity and toughness of polymeric hydrogels. *Macromolecules, 36*(12), 4582–4588.

Mørch, Ý. A., Donati, I., Strand, B. L., & Skjåk-Bræk, G. (2007). Molecular engineering as an approach to design new functional properties of alginate. *Biomacromolecules, 8*(9), 2809–2814.

Mørch, Y. A., Holtan, S., Donati, I., Strand, B. L., & Skjåk-Bræk, G. (2008). Mechanical properties of C-5 epimerized alginates. *Biomacromolecules, 9*(9), 2360–2368.

Marsich, E., Travan, A., Feresini, M., Lapasin, R., Paoletti, S., & Donati, I. (2013). Polysaccharide-based polyanion-polycation-polyanion ternary systems in the concentrated regime and hydrogel form. *Macromolecular Chemistry and Physics, 214*(12), 1309–1320.

Nilsen-Nygaard, J., Strand, S., Vårum, K. M., Draget, K., & Nordgård, C. (2015). Chitosan: Gels and interfacial properties. *Polymers, 7*(3), 552–579.

Racine, L., Texier, I., & Auzély-Velty, R. (2017). Chitosan-based hydrogels: Recent design concepts to tailor properties and functions. *Polymer International, 66*(7), 981–998.

Sacco, P., Borgogna, M., Travan, A., Marsich, E., Paoletti, S., Asaro, F., ... Donati, I. (2014). Polysaccharide-based networks from homogeneous chitosan-Tripolyphosphate hydrogels: Synthesis and characterization. *Biomacromolecules, 15*(9), 3396–3405.

Sacco, P., Paoletti, S., Cok, M., Asaro, F., Abrami, M., Grassi, M., & Donati, I. (2016). Insight into the ionotropic gelation of chitosan using tripolyphosphate and pyrophosphate as cross-linkers. *International Journal of Biological Macromolecules, 92*,

476–483.

Sacco, P., Brun, F., Donati, I., Porrelli, D., Paoletti, S., & Turco, G. (2018). On the correlation between the microscopic structure and properties of phosphate-cross-linked chitosan gels. *ACS Applied Materials & Interfaces, 10*(13), 10761–10770.

Sen, S., Engler, A. J., & Discher, D. E. (2009). Matrix strains induced by cells: Computing how far cells can feel. *Cellular and Molecular Bioengineering, 2*(1), 39–48.

Skjåk-Bræk, G., Grasdalen, H., & Smidsrød, O. (1989). Inhomogeneous polysaccharide ionic gels. *Carbohydrate Polymers, 10*(1), 31–54.

Smidsrød, O., & Haug, A. (1972). Properties of poly(1,4-hexuronates) in the gel state: II. Comparison of gels of different chemical composition. *Acta Chemica Scandinavica, 26*, 79–88.

Sorlier, P., Denuzière, A., Viton, C., & Domard, A. (2001). Relation between the degree of acetylation and the electrostatic properties of chitin and chitosan. *Biomacromolecules, 2*(3), 765–772.

Soskey, P. R., & Winter, H. H. (1984). Large step shear strain experiments with parallel-disk rotational rheometers. *Journal of Rheology, 28*(5), 625–645.

Supper, S., Anton, N., Seidel, N., Riemenschnitter, M., Schoch, C., & Vandamme, T. (2013). Rheological study of chitosan/polyol-phosphate systems: Influence of the polyol part on the thermo-Induced gelation mechanism. *Langmuir, 29*(32), 10229–10237.

Tømmeraas, K., Vårum, K. M., Christensen, B. E., & Smidsrød, O. (2001). Preparation and characterisation of oligosaccharides produced by nitrous acid depolymerisation of chitosans. *Carbohydrate Research, 333*(2), 137–144.

Vårum, K. M., Anthonsen, M. W., Grasdalen, H., & Smidsrød, O. (Anthonsen, Grasdalen, and Smidsrød, 1991a). 13C-n.m.r: Studies of the acetylation sequences in partially N-deacetylated chitins (chitosans). *Carbohydrate Research, 217*, 19–27.

Vårum, K. M., Anthonsen, M. W., Grasdalen, H., & Smidsrød, O. (Anthonsen, Grasdalen, and Smidsrød, 1991b). Determination of the degree of N-acetylation and the distribution of N-acetyl groups in partially N-deacetylated chitins (chitosans) by high-field n.m.r. spectroscopy. *Carbohydrate Research, 211*(1), 17–23.

Zhang, J., Daubert, C. R., & Allen Foegeding, E. (2007). A proposed strain-hardening mechanism for alginate gels. *Journal of Food Engineering, 80*(1), 157–165.